FEBS Letters 587 (2013) 2506–2511

FEBS Letters

journal homepage: www.FEBSLetters.org

The CH2 domain of CBP/p300 is a novel zinc finger

Sangho Park, Maria A. Martinez-Yamout, H. Jane Dyson, Peter E. Wright *

Department of Integrative Structural and Computational Biology and Skaggs Institute of Chemical Biology, The Scripps Research Institute, 10550 North Torrey Pines Road, La Jolla, CA 92037, USA

ARTICLE INFO

Article history:
Received 13 May 2013
Revised 17 June 2013
Accepted 24 June 2013
Available online 4 July 2013

Edited by Christian Griesinger

Keywords:
CBP
p300
Plant homeodomain
Zinc finger
Bromodomain

ABSTRACT

The transcriptional co-regulator CBP (CREB-binding protein) has a highly conserved cysteine/histidine-rich region (CH2) whose structure and function remain uncharacterized. Using nuclear magnetic resonance (NMR spectroscopy), sequence alignment, mass spectrometry, and mutagenesis, we show that the CH2 domain is not a canonical plant homeodomain (PHD) finger, as previously proposed, but binds an additional zinc atom through the region N-terminal to the putative PHD motif. The CH2 domain and the preceding bromodomain interact and mutually stabilize each other, implying a cooperative function. We tested the hypothesis that the bromodomain and the CH2 domain can interact with histones, but found that the CH2 does not participate in histone-recognition.

Structured summary of protein interactions:
H4 binds to CBP by peptide array (View Interaction: 1, 2).

1. Introduction

CREB-binding protein (CBP) and its paralog p300 are transcriptional co-regulators that integrate numerous signal transduction pathways and play critical roles in various cellular processes such as cell proliferation, differentiation, apoptosis, and DNA repair [1]. Defects in CBP/p300 are implicated in a number of human diseases including certain types of leukemia and lymphoma, gastric and colorectal carcinomas, and congenital malformation syndromes [2–5]. The biological functions of CBP and p300 are associated with their ability to interact with a large number of proteins through multiple protein-interaction domains as well as from the acetyltransferase activity associated with their histone acetyl transferase (HAT) domains [6–8].

CBP and p300 have three cysteine/histidine rich zinc-binding domains, termed CH1, CH2 and CH3 [9]. Although the CH1 and CH3 domains have been well-characterized both structurally and functionally, the structure and function of the cysteine/histidine-rich region 2 (CH2) domain remains largely unknown. Based on the presence of a conserved C4HC3 motif [10], it has been proposed that the CH2 domain of CBP/p300 contains a consensus plant homeodomain (PHD)-type zinc finger [11]. The CH2 domain of CBP is located between the bromodomain (BRD), which functions as an acetyl-lysine binding domain [12,13], and the HAT domain and is essential for acetylation of histones both *in vitro* and *in vivo* [11,14]. It has been suggested that the BRD and the CH2 domain of p300 bind nucleosomes [15]. BRD and PHD domains are frequently fused to each other and function in concert to read multivalent histone marks [16]. However, it has not been established whether the CH2 domain of CBP/p300 can recognize epigenetic histone marks, although many other PHD fingers have been shown to recognize histone H3 with methylation of K4 or K9 or with acetylation of K14 [17,18]. Whereas in most PHD–BRD cassettes in the human proteome, the PHD is N-terminal to the BRD, in CBP/p300, the PHD is preceded by the BRD and a cysteine rich linker.

Here we show, by sequence alignment, mass spectrometry, and mutagenesis, that the CH2 domain of CBP does not contain a canonical PHD domain but is an atypical zinc finger that binds three zinc atoms. We report nuclear magnetic resonance (NMR) and circular dichroism (CD) data that demonstrate that the BRD and CH2 domains form an autonomous structural unit and that each domain stabilizes the other. Using histone peptide arrays, we also show that the BRD binds to histone H2B and H4 acetylation marks whereas the CH2 domain does not recognize any additional histone modifications.

Abbreviations: CBP, CREB-binding protein; BRD, bromodomain; PHD, plant homeodomain; CH2, cysteine/histidine-rich region 2; HAT, histone acetyl transferase; NMR, nuclear magnetic resonance; HSQC, heteronuclear single-quantum coherence; CD, circular dichroism

* Corresponding author. Fax: +1 858 784 9822.
E-mail address: wright@scripps.edu (P.E. Wright).

0014-5793/$36.00 © 2013 Federation of European Biochemical Societies. Published by Elsevier B.V. All rights reserved.
http://dx.doi.org/10.1016/j.febslet.2013.06.051

2. Materials and methods

2.1. Preparation of proteins

The coding sequences for the BRD (residues 1079–1198) and BRD–CH2 region (1079–1317) of mouse CBP were cloned into the pGEX-4T2 vector between BamHI and XhoI sites. The GST-tagged proteins were expressed in *Escherichia coli* BL21 (DE3) cells by IPTG induction at 15°C. The proteins were initially purified by affinity chromatography on a Glutathione Sepharose 4B column followed by size-exclusion chromatography on a Sephacryl S-100 column. GST-tagged proteins were used for the binding assays on MODified™ Histone Peptide Arrays. For other experiments, the GST tag was removed by thrombin cleavage and the resulting proteins were purified using Glutathione Sepharose 4B and Sephacryl S-100 chromatography columns. Potential zinc ligands in the BRD–CH2 domain construct were mutated to Ser or Ala (C1200S, C1201S, C1213S, C1214S, C1220S, H1236A, H1292A, and H1298A) using QuikChange Site-Directed Mutagenesis Kits. Mutant proteins were expressed and purified by the same protocol as for the wild-type protein.

The CH2 domain (residues 1192–1318) and the CH2 domain with N-terminal truncation (CH2ΔN, residues 1225–1315) of mouse CBP were cloned into the pET-21a vector between NdeI and BamHI sites. The proteins were expressed in *E. coli* BL21 (DE3) [DNAY] host cells by IPTG induction at 20°C and purified by ion-exchange chromatography using Q-Sepharose and size-exclusion chromatography using Sephacryl S-100.

2.2. NMR spectroscopy

NMR data were collected on Bruker 800, 750, and 500 MHz spectrometers at 30°C unless otherwise specified. A 0.6 mM uniformly ^{15}N,^{13}C-labeled BRD sample in NMR buffer (25 mM Tris–HCl, pH 7.0, 50 mM NaCl, 1 mM DTT in 90% H_2O:10% ^2H_2O) was used to record two-dimensional (2D) HSQC and three-dimensional (3D) HNCA spectra. Backbone resonances of the BRD were assigned from a 3D HNCA experiment at 20°C, assisted by the deposited assignment data (Biological Magnetic Resonance Data Bank id: 17392). A sample of 1 mM uniformly ^{15}N,^{13}C,^{2}H-labeled BRD–CH2 in NMR buffer (supplemented with 50 μM $ZnSO_4$) was used to obtain 2D TROSY, 3D HNCA, 3D HNCACB, 3D CBCA(CO)NH, and 3D HNCO for backbone assignments. ^1H–^{15}N HSQC spectra were also acquired for 246 μM CH2 and 134 μM CH2ΔN samples in NMR buffer supplemented with 50 μM $ZnSO_4$. For the BRD–CH2 mutants, ^1H–^{15}N HSQC and ^1H–^{15}N TROSY spectra were acquired using 200–600 μM samples. All NMR data were processed and analyzed using NMRPipe [19] and Sparky [20].

2.3. Circular dichroism spectroscopy

Circular dichroism (CD) spectra were recorded for 10 μM BRD and 5 μM BRD–CH2 in 10 mM MES buffer (pH 6.7) containing 0.5 mM DTT using an Aviv model 202 CD spectrometer. Thermal denaturation was monitored by recording the CD signal at 208 nm as a function of increasing temperature from 20 to 100°C. Melting temperatures (T_ms) were determined by fitting the raw data to the Boltzmann sigmoidal equation using QtiPlot software. For the two phase thermal denaturation curve of BRD–CH2, the data from 20 to 60°C and the data from 55 to 100°C were separately used for fitting.

2.4. Electrospray ionization-mass spectrometry (ESI-MS)

Purified BRD–CH2 was completely desalted using a NAP-10 column. 150 μM BRD–CH2 in 10 mM ammonium acetate was directly injected into an Agilent 1100 Series ESI-MS spectrometer. MS data was acquired in positive ion mode using capillary voltage of 5000 V and fragmentator voltage of 175 V. The mass spectrum collected for m/z range of 1000–2500 was deconvoluted using Chemstation software.

2.5. NMR studies of BRD–CH2 interactions with a histone H2BK15Ac peptide

A histone H2B peptide (residues 1–20) acetylated at K15 was prepared by solid-phase synthesis on a Perseptive Biosystems synthesizer using Fmoc chemistry. The H2BK15Ac peptide was purified by reversed phase HPLC. NMR experiments were performed by acquiring 2D TROSY spectra of 0.1 mM ^{15}N-labeled BRD–CH2 in NMR buffer containing 50 μM $ZnSO_4$ in the presence or absence of 1 mM H2BK15Ac peptide.

2.6. Histone binding assay

MODified™ Histone Peptide arrays were purchased from Active Motif. Arrays were first blocked by immersing in 10 mM Tris–HCl, pH 7.4, 0.05% Tween 20, 150 mM NaCl, and 5% (w/v) non-fat dried milk, and then incubated with 50 μM GST-BRD, 50 μM GST-BRD–CH2, or 50 μM GST-BRD–CH2 with 1 mM H2BK15Ac peptide in 25 mM Tris–HCl, pH 8.0, 100 mM NaCl, 1 mM DTT, and 50 μM $ZnSO_4$. Arrays were then treated with HRP-conjugated anti-GST antibody (GenScript). Signals were detected using enhanced chemiluminescence and captured by the FluorChem 8900 Imaging System (AlphaInnotech).

3. Results

3.1. The BRD and CH2 domains of CBP are associated

Two CBP constructs, one consisting of the isolated BRD and the other containing both the BRD and the CH2 domains (BRD–CH2), were expressed and labeled uniformly with ^{13}C and ^{15}N for NMR spectroscopy. The backbone amide resonances of both constructs were assigned using conventional triple-resonance experiments. A 2D HSQC spectrum of the BRD and a 2D TROSY spectrum of the BRD–CH2 construct with assignments are shown in the Supplementary Fig. S1. We initially aimed to determine the structure of the BRD–CH2 construct, but the NMR data are of insufficient quality for structure determination. About 10% of backbone resonances are missing and side-chain assignments could not be made, presumably due to a dynamic exchange process that broadens the NMR signals and degrades the spectral resolution. However, we could obtain important information about the organization of the BRD and CH2 domains from the available backbone assignments. A number of amide resonances of the BRD undergo large changes in chemical shift or broaden out in the BRD–CH2 construct (Fig. 1A and Supplementary Fig. S1C), showing that the two domains associate with each other rather than behaving as independent beads on a string. The interaction site has been mapped to the opposite end of the BRD helical bundle from the binding site for acetyl-lysine peptides (Fig. 1B).

We employed CD spectroscopy to investigate the thermal stability of the BRD in the presence and absence of the CH2 domain. CD spectra of the BRD and BRD–CH2 constructs were measured at 208 nm, which is a characteristic minimum for α-helical proteins, as a function of increasing temperature. The BRD shows a typical thermal denaturation pattern for a single domain with a T_m of 41°C (Fig. 2A). In contrast, the BRD–CH2 construct undergoes two phase denaturation, with T_ms of 49°C and 72°C (Fig. 2B). The first phase of denaturation of the BRD–CH2 occurs 8°C higher than

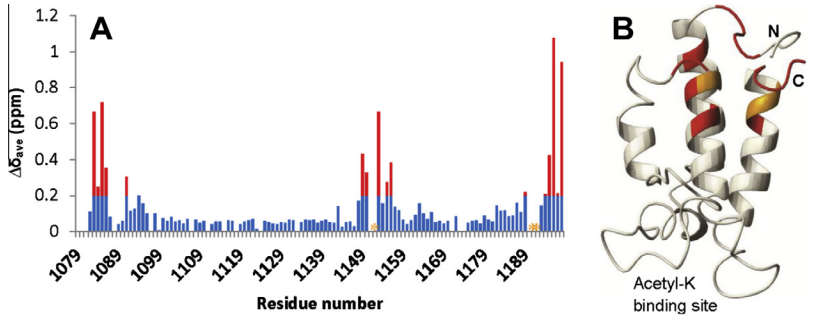

Fig. 1. The BRD and the CH2 domain interact with each other. (A) A plot of chemical shift differences ($\Delta\delta_{ave}$) of the backbone H^N and N resonances of the BRD of CBP between the isolated BRD and BRD–CH2. The weighted average chemical shift change was calculated from the equation $\Delta\delta_{ave} = \{(\Delta\delta N/5)^2 + (\Delta\delta H^N)^2\}^{1/2}$. Red bars indicate changes in $\Delta\delta_{ave}$ greater than 0.2. Residues whose resonances are completely broadened out due to the interaction are marked by orange asterisks. (B) Residues that exhibit significant perturbation are mapped on the structure of the BRD (PDB id: 1JSP) using the same color code as in (A).

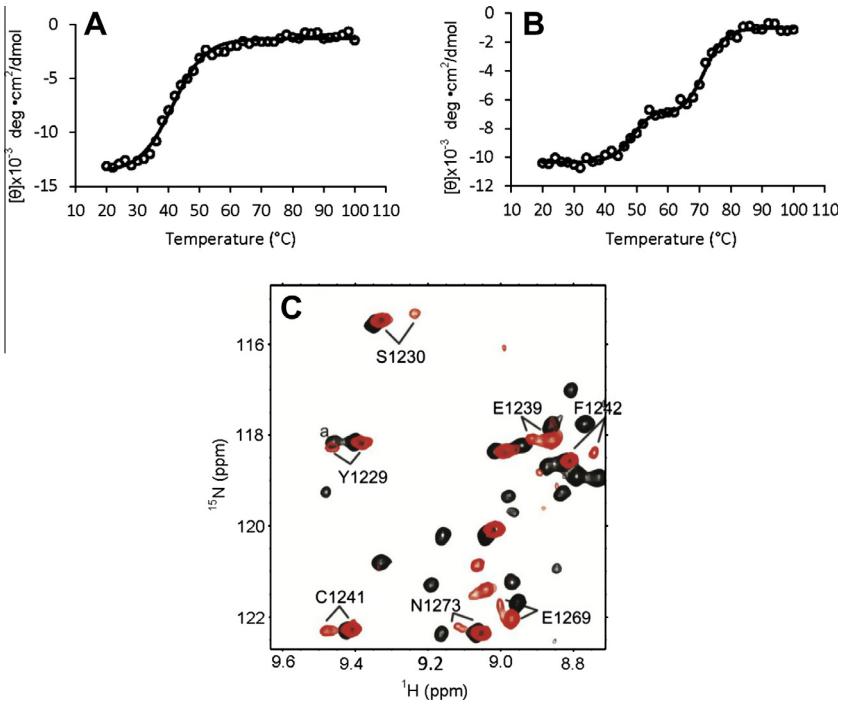

Fig. 2. The BRD and the CH2 domain are more stable in BRD–CH2 than the isolated domains. Thermal denaturation of the BRD (A) and BRD–CH2 (B) measured by CD spectroscopy. The CD values measured at 208 nm are plotted against temperature ranging from 20 to 100°C. Open circles are raw data while the solid lines show the fitted values using a sigmoidal curve. (C) An overlay of a selected region of the HSQC spectra of the isolated CH2 domain (red) and BRD–CH2 (black), showing residues observed as two peaks only in the spectrum of the CH2 domain. [a]This peak in BRD–CH2 is from N1163.

for the isolated BRD, suggesting that the BRD is stabilized against thermal denaturation by fusion to the CH2 domain. The second transition is most likely associated with denaturation of the CH2 domain, which we expect to have a high denaturation temperature due to the coordination of zinc. Attempts to monitor thermal denaturation of the isolated CH2 domain by CD were unsuccessful. However, ^1H–^{15}N HSQC spectra provide strong evidence that the CH2 domain is stabilized by fusion to the BRD. Several residues, including Y1229, S1230, E1239, C1241, F1242, E1269, and N1273, exhibit split cross peaks in the HSQC spectrum of the isolated CH2 domain, which implies that these residues adopt two different conformations (Fig. 2C). Each of these residues gives rise to a single cross peak in the HSQC spectrum of the BRD–CH2 construct. Additionally, the cross peaks of many residues are broadened in the HSQC spectrum of the isolated CH2 domain due to conformational exchange, but are readily observed in the spectrum of the BRD–CH2 construct. Thus, both the BRD and CH2 domain structures are mutually stabilized in the BRD–CH2 fusion construct relative to the isolated domains.

3.2. The CH2 domain of CBP is a non-canonical zinc finger that binds three zinc atoms

It has been proposed that residues 1233–1315 of the CH2 domain of CBP/p300 constitute a PHD finger, which binds two zinc atoms [10,11]. Unlike the canonical PHD motif, which forms a stable and independently folded globular structure, the C4HC3 region of the CH2 domain does not fold independently. The entire CH2 domain, including the 33 amino acids N-terminal to the C4HC3 motif of the putative PHD zinc finger, is required for formation of a folded structure. The ^1H–^{15}N HSQC spectrum of CH2ΔN, which contains only the C4HC3 motif, is poorly dispersed and many cross peaks

are broadened beyond detection, implying that the protein is not well folded (Fig. 3A). In contrast, the full-length CH2 domain (residues 1192–1318) shows a well-dispersed ^{1}H–^{15}N HSQC spectrum characteristic of a folded protein (Fig. 3A). In addition, CH2ΔN aggregated through mixed-disulfide formation which could be reversed by adding fresh reducing agent, suggesting that some of the seven cysteines of CH2ΔN are not properly participating in zinc coordination. From these results, we conclude that the N-terminal 33 amino acid extension to the C4HC3 motif is an integral part of the CH2 domain structure. ESI-MS analysis of the BRD–CH2 construct demonstrated the presence of three zinc atoms (Fig. 3B). The difference between the observed mass (28 465 Da) and the mass calculated from the amino acid sequence (28,276 Da) is 189 Da, which corresponds to the mass of three zinc atoms. Therefore, the CH2 domain of CBP binds three zinc atoms and the N-terminal extension of the CH2 domain is necessary for proper coordination of zinc.

Alignment of available CBP/p300 sequences showed the presence of four invariant cysteine residues in the N-terminal extension preceding the C4HC3 motif of the CH2 domain (Fig. 4). These residues are absolutely conserved in CBP homologs ranging from single-celled organisms to plants and animals. In order to confirm that only the conserved cysteines and histidine are involved in zinc binding, a number of single amino acid mutants were prepared. Three of these mutants, C1213S, H1236A, and H1298A, which are not conserved, expressed well as soluble

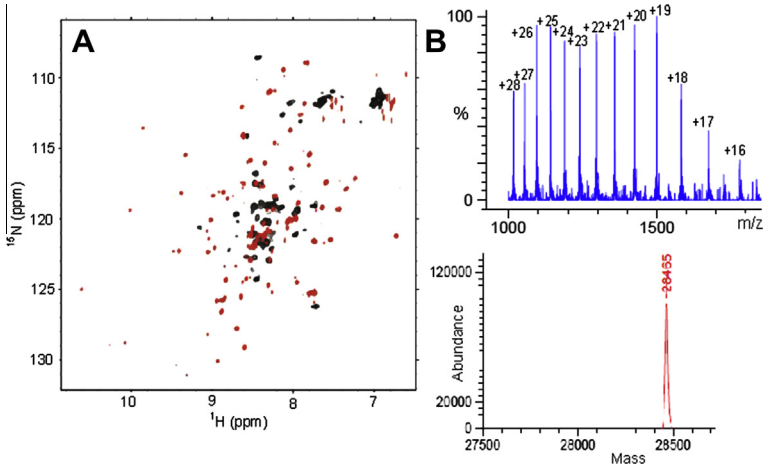

Fig. 3. The CH2 domain of CBP requires three zinc atoms to fold properly. (A) An overlay of the ^{1}H–^{15}N HSQC spectra of the CH2ΔN (black) and the full-length CH2 domain (red). (B) ESI-MS spectrum of the BRD–CH2 construct (top) and the deconvoluted spectrum that shows a component with a mass of 28 465 Da (bottom).

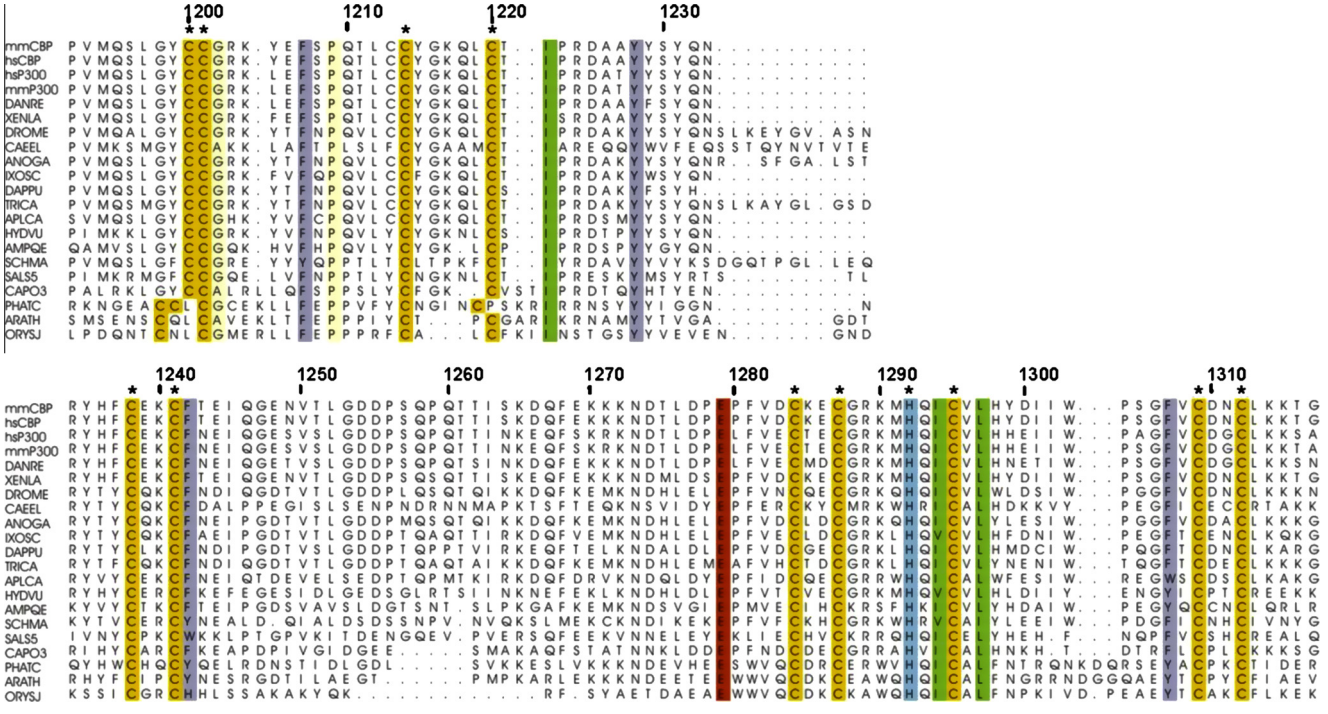

Fig. 4. Sequence alignment of the CH2 domains of CBP and p300 homologs. Residues numbers of mouse CBP are shown above the sequence. Completely conserved residues throughout species are colored by residue types. Residues proposed to coordinate zinc atoms are marked by asterisks. Sequences included are CBP/P300_MOUSE, CBP/P300_HUMAN, XP_001332718.3, NP_001088637.1, Q9W321_DROME, CBP1_CAEEL, XP_311133.5, XP_002411559.1, EFX66192.1, XP_782558.3, EFA02517.1, NP_001191640.1, XP_002156492.2, XP_003383601.1, XP_002572380.1, EGD72148.1, XP_004347654.1, XP_002179989.1, HAC1_ARATH, HACL3_ORYSJ.

recombinant proteins just like the wild-type protein. Subsequent NMR experiments on these mutants revealed that they are correctly folded and give similar HSQC spectra to that of the wild-type protein, proving that these residues are not involved in zinc-binding (Supplementary Fig. S2). In contrast, *E. coli* expression of other mutants, C1200S, C1201S, C1214S, C1220S, and H1292A, in which invariant cysteine or histidine residues were replaced, resulted in mostly insoluble recombinant proteins. We interpret this as evidence of misfolding due to substitution of ligands involved in zinc binding. Assuming four ligand residues are necessary to bind each zinc atom, all 11 invariant cysteines and the one invariant histidine are required for binding three zinc atoms.

We used the available resonance assignments and the program TALOS+ [21] to identify the secondary structure of the CH2 domain for comparison with canonical PHD structures. The secondary structure of the CH2 domain, within the BRD–CH2 construct, is summarized in Supplementary Fig. S3. Canonical PHD motifs bind two zinc atoms in a cross-brace topology and have a characteristic antiparallel β-sheet formed by two short β-strands [17]. The secondary structure of the C4HC3 region of the CH2 domain differs from the canonical PHD in three ways. Firstly, residues E1239–E1244 of the C4HC3 region, spanning the first zinc-binding CXXC module, form a well-defined helix that is not found in the PHD motif. Secondly, residues R1289-H1292 of CBP, which would form one of the strands of the characteristic β-sheet of a PHD motif, do not form a β-strand in the CH2 domain. Finally, residues G1247-D1277 form a long structured insertion in place of a short loop connecting the first pair of CXXC modules in the canonical PHD motif. Thus, the C4HC3 region of CBP differs from the canonical PHD motif in both its secondary structure and its ability to fold as an independent domain.

3.3. The BRD binds acetylated histone H2B and H4 peptides

Many PHD fingers have been shown to be readers of epigenetic histone marks [17]. To determine whether the CH2 domain of CBP functions in recognition of modified histones, we screened for binding using MODified™ Histone Peptide arrays from Active Motif. We used the GST-tagged BRD–CH2 construct for the assay and compared the results with binding data for the isolated BRD using a GST-BRD construct. The BRD–CH2 was observed to bind preferentially to several acetylated histone H4 and H2B peptides (Fig. 5A). However, the isolated BRD binds to the same set of H4 and H2B peptides (Fig. 5A). We also carried out a binding assay of the BRD–CH2 using a histone H2B peptide with acetylation at K15 (H2BK15Ac) in the assay buffer to see if the BRD and the CH2 domains bind cooperatively to modifications on two separate histone peptides. In this array, the BRD–CH2 did not recognize an additional modification and, instead, its binding to the acetylated H2B and H4 peptides on the array became weaker because the immobilized histone peptides have to compete with the free H2BK15Ac peptide. In confirmation of the results obtained with histone arrays, only the BRD HSQC cross peaks were perturbed upon addition of the H2BK15Ac peptide into ^{15}N-labeled BRD–CH2, indicating that the CH2 domain does not participate in histone binding (Supplementary Fig. S4). Taken together, our data indicate that the CH2 domain of CBP does not read an additional epigenetic mark.

4. Discussion

Our data provide strong evidence that the CH2 domain of CBP is not a PHD zinc finger but is a non-canonical zinc finger that binds three zinc atoms. The entire CH2 sequence is required for formation of a stable folded structure in the presence of zinc. The N-terminal extension to the putative PHD finger, which was previously regarded as a linker between the BRD and PHD, appears to be an integral part of the CH2 zinc finger, providing four additional ligands that accommodate one zinc atom. Zinc fingers of MLL1 and AF10, which were initially considered as PHD fingers, have also a cysteine/histidine-enriched N-terminal extension to the PHD-like motif [22,23]. These zinc fingers, arranging cysteine and histidines as HC5HC2H, are now classified as a PHD-like zinc binding domain in the PFAM database. However, the CH2 domain of CBP has no sequence similarity with those PHD-like zinc binding domains. Since no PHD finger has been reported to have an extension that binds an additional zinc atom, our results strongly suggest that the CH2 domain of CBP/p300 is a novel type of zinc finger.

The CH2 domain precedes the HAT domain in CBP homologs ranging from single-celled organisms to plants and higher eukaryotes. The N-terminus of CH2 that includes the additional zinc-binding cysteine residues contains a previously identified motif (PFAM DUF902), which appears at the C-terminus of BRD domains in animal, but not plant, CBP homologs. We show that the DUF902 motif is an integral part of the CH2 domain. The fact that the CH2 domain is always associated with the HAT domain suggests that the CH2

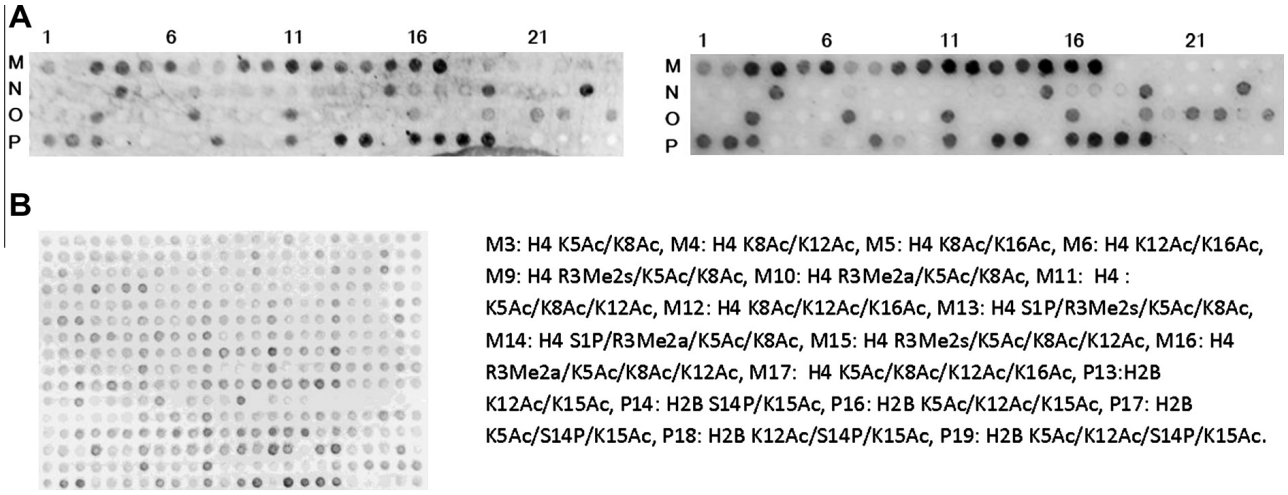

Fig. 5. The BRD binds to H2B and H4 with acetylation whereas the CH2 domain does not recognize any additional mark. (A) A selected region of the Modified™ Histone Peptide array of BRD–CH2 (left) and the BRD (right). Post-translational modifications for the spots with a strong signal are shown below. Ac: acetylation, P: phosphorylation, Me2s: symmetric di-methylation, Me2a: asymmetric di-methylation. A full-region of the arrays and the complete list of modifications are shown in Supplementary data. (B) An array of BRD–CH2 in the presence of the H2BK15Ac peptide.

domain plays an important functional role in HAT domain activity. A previous study has shown that the CH2 domain of CBP is essential for *in vitro* acetyltransferase activity and transcriptional activity and mutations in the CH2 domain are associated with loss of acetyltransferase activity in Rubinstein-Taybi syndrome [11,14]. Based on our finding that the BRD and the CH2 domain of CBP associate with each other, these two domains may also function in a cooperative manner. Although it has been proposed that both the BRD and the CH2 domain of p300 can interact with nucleosomes that have a high degree of acetylation [15], we were unable to find any evidence to support a potential role for the CH2 domain in recognition of epigenetic histone marks. However, we cannot exclude the possibility that the CH2 domain may bind to the nucleosome core instead of tails, which should be addressed by further studies.

Acknowledgements

This work was supported by grant R01 CA096865 to P.E.W. from the National Institutes of Health and by the Skaggs Institute for Chemical Biology.

Appendix A. Supplementary data

Supplementary data associated with this article can be found, in the online version, at http://dx.doi.org/10.1016/j.febslet.2013.06.051.

References

[1] Goodman, R.H. and Smolik, S. (2000) CBP/p300 in cell growth, transformation, and development. Genes Dev. 14 (13), 1553–1577.
[2] Mullighan, C.G. et al. (2011) CREBBP mutations in relapsed acute lymphoblastic leukaemia. Nature 471 (7337), 235–239.
[3] Pasqualucci, L. et al. (2011) Inactivating mutations of acetyltransferase genes in B-cell lymphoma. Nature 471 (7337), 189–195.
[4] Giles, R.H., Peters, D.J. and Breuning, M.H. (1998) Conjunction dysfunction: CBP/p300 in human disease. Trends Genet. 14 (5), 178–183.
[5] Iyer, N.G., Ozdag, H. and Caldas, C. (2004) P300/CBP and cancer. Oncogene 23 (24), 4225–4231.
[6] Kalkhoven, E. (2004) CBP and p300: HATs for different occasions. Biochem. Pharmacol. 68 (6), 1145–1155.
[7] Shiama, N. (1997) The p300/CBP family: integrating signals with transcription factors and chromatin. Trends Cell Biol. 7 (6), 230–236.
[8] Vo, N. and Goodman, R.H. (2001) CREB-binding protein and p300 in transcriptional regulation. J. Biol. Chem. 276 (17), 13505–13508.
[9] Borrow, J. et al. (1996) The translocation t(8;16) (p11;p13) of acute myeloid leukaemia fuses a putative acetyltransferase to the CREB-binding protein. Nat. Genet. 14 (1), 33–41.
[10] Aasland, R., Gibson, T.J. and Stewart, A.F. (1995) The PHD finger: implications for chromatin-mediated transcriptional regulation. Trends Biochem. Sci. 20 (2), 56–59.
[11] Kalkhoven, E. et al. (2002) The PHD type zinc finger is an integral part of the CBP acetyltransferase domain. Mol. Cell. Biol. 22 (7), 1961–1970.
[12] Zeng, L. et al. (2008) Structural basis of site-specific histone recognition by the bromodomains of human coactivators PCAF and CBP/p300. Structure 16 (4), 643–652.
[13] Zeng, L. and Zhou, M.M. (2002) Bromodomain: an acetyl-lysine binding domain. FEBS Lett. 513 (1), 124–128.
[14] Kalkhoven, E. et al. (2003) Loss of CBP acetyltransferase activity by PHD finger mutations in Rubinstein-Taybi syndrome. Hum. Mol. Genet. 12 (4), 441–450.
[15] Ragvin, A. et al. (2004) Nucleosome binding by the bromodomain and PHD finger of the transcriptional cofactor p300. J. Mol. Biol. 337 (4), 773–788.
[16] Ruthenburg, A.J. et al. (2007) Multivalent engagement of chromatin modifications by linked binding modules. Nat. Rev. Mol. Cell Biol. 8 (12), 983–994.
[17] Sanchez, R. and Zhou, M.M. (2011) The PHD finger: a versatile epigenome reader. Trends Biochem. Sci. 36 (7), 364–372.
[18] Mansfield, R.E. et al. (2011) Plant homeodomain (PHD) fingers of CHD4 are histone H3-binding modules with preference for unmodified H3K4 and methylated H3K9. J. Biol. Chem. 286 (13), 11779–11791.
[19] Delaglio, F. et al. (1995) NMRPipe: a multidimensional spectral processing system based on UNIX pipes. J. Biomol. NMR 6 (3), 277–293.
[20] Goddard, T.D. and Kneller, D. (2006). SPARKY 3, University of California, California.
[21] Shen, Y. et al. (2009) TALOS+: a hybrid method for predicting protein backbone torsion angles from NMR chemical shifts. J. Biomol. NMR 44 (4), 213–223.
[22] Fair, K. et al. (2001) Protein interactions of the MLL PHD fingers modulate MLL target gene regulation in human cells. Mol. Cell. Biol. 21 (10), 3589–3597.
[23] Linder, B. et al. (2000) Biochemical analyses of the AF10 protein: the extended LAP/PHD-finger mediates oligomerisation. J. Mol. Biol. 299 (2), 369–378.